Searches for $B^0 \to K^+\pi^-\tau^+\tau^-$ and $B_s^0 \to K^+K^-\tau^+\tau^-$ Decays

R. Aaij *et al.*[*]
(LHCb Collaboration)

(Received 16 October 2025; accepted 24 March 2026; published 5 May 2026)

The first searches for $B^0 \to K^+\pi^-\tau^+\tau^-$ and $B_s^0 \to K^+K^-\tau^+\tau^-$ decays at the LHCb experiment are conducted with pp collision data corresponding to an integrated luminosity of 5.4 fb^{-1}. The tau leptons are reconstructed using the $\tau^+ \to \mu^+\bar{\nu}_\tau\nu_\mu$ decay and the results are presented in bins of $K^+\pi^-$ or K^+K^- mass. No signal is observed and upper limits are set on the branching fractions. The searches result in the first upper limits for $B^0 \to K^+\pi^-\tau^+\tau^-$ decays outside the $K^*(892)^0$ region in $K^+\pi^-$ mass and the first limits for $B_s^0 \to K^+K^-\tau^+\tau^-$ decays. The searches are recast into limits on the decays $B^0 \to K^*(892)^0\tau^+\tau^-$ and $B_s^0 \to \phi(1020)\tau^+\tau^-$, yielding 2.8×10^{-4} (2.5×10^{-4}) and 4.7×10^{-4} (4.1×10^{-4}) at the 95% (90%) confidence level, respectively. For the decay $B^0 \to K^*(892)^0\tau^+\tau^-$, this result improves on the current best upper limit by an order of magnitude.

DOI: 10.1103/y968-44v8

Over the past decade, analyses of flavor-changing neutral current decays with the quark-level transition $b \to s\mu^+\mu^-$ have shown consistent discrepancies with standard model (SM) expectations [1–10]. At the same time, measurements of branching-fraction ratios in tree-level $b \to c\ell^-\bar{\nu}_\ell$ decays, with final states containing either a tau or a light lepton, $R(D^{(*)})$, have shown deviations from lepton flavor universality [11–22].

Models of physics beyond the SM that account for these discrepancies predict enhancements of several orders of magnitude in the branching fractions of flavor-changing neutral current $b \to s\tau^+\tau^-$ transitions [23–31]. Large increases of these branching fractions may also be expected solely within the context of explaining the $b \to s\mu^+\mu^-$ anomalies [32,33].

Standard model predictions have been made for the branching fractions of $B^0 \to K^{*0}\tau^+\tau^-$ and $B_s^0 \to \phi\tau^+\tau^-$ decays that are both of order 10^{-7} [27]. Throughout this Letter, charge conjugate processes are implied and the symbols K^{*0} and ϕ refer to the specific states $K^*(892)^0$ and $\phi(1020)$, respectively. In a weak effective theory, the coupling strength of the vector (axial vector) operators is given by the Wilson coefficients $C^{\tau\tau}_{9(10)}$. Beyond-the-SM effects may be introduced via a shift, Δ, such that $C_9^{\tau\tau} = C_9^{\mathrm{SM}} - \Delta$ and $C_{10}^{\tau\tau} = C_{10}^{\mathrm{SM}} + \Delta$, where C_9^{SM} is 4.1 and C_{10}^{SM} is −4.3 [27]. If $\Delta \gg C_{9,10}^{\mathrm{SM}}$ the branching fractions are given by [27]

$$\mathcal{B}(B^0 \to K^{*0}\tau^+\tau^-) = (10.1 \pm 0.8) \times 10^{-9} \times \Delta^2,$$
$$\mathcal{B}(B_s^0 \to \phi\tau^+\tau^-) = (9.1 \pm 0.5) \times 10^{-9} \times \Delta^2. \quad (1)$$

Models with $\Delta = O(100)$, corresponding to branching fractions of order 10^{-5}, are consistent with the current $R(D^{(*)})$ results. The observation of such large branching fractions for these decays would unambiguously indicate the presence of physics beyond the SM. Searches for $B^0_{(s)} \to \tau^+\tau^-$ [34], $B^+ \to K^+\tau^+\tau^-$ [35] and $B^0 \to K^{*0}\tau^+\tau^-$ [36,37] decays have previously been conducted, resulting in upper limits on the branching fractions of order 10^{-3}. In the most recent of these searches, the Belle II Collaboration constrains $\mathcal{B}(B^0 \to K^{*0}\tau^+\tau^-) < 1.8 \times 10^{-3}$ at 90% confidence level (CL), reconstructing tau candidates via their decays to single-muon, electron, charged pion, and charged ρ final states [37]. Searches for rescattering effects in $B^0 \to K^{*0}\mu^+\mu^-$ [38] constrain $|C_9^{\tau\tau}| < 600$ at 95% CL [8].

In this Letter, two new LHCb searches for $b \to s\tau^+\tau^-$ decays are performed using the modes $B^0 \to K^+\pi^-\tau^+\tau^-$ and $B_s^0 \to K^+K^-\tau^+\tau^-$. In both cases the tau leptons are reconstructed using the decay $\tau^+ \to \mu^+\nu_\mu\bar{\nu}_\tau$. Although the two searches reconstruct different final states, the analysis strategy is common between them. Reconstructing a final state with two charged hadrons allows the location of the $B^0_{(s)}$ decay vertex to be determined from the intersection of the hadron tracks. Knowledge of this vertex location facilitates efficient background suppression and partial reconstruction of the b-hadron decay topology. Furthermore, the large branching fraction of the $\tau^+ \to \mu^+\nu_\mu\bar{\nu}_\tau$ decay, and the high efficiency of muon reconstruction at LHCb [39], result in large samples of tau candidates for these studies.

[*]Full author list given at the end of the Letter.

Published by the American Physical Society under the terms of the Creative Commons Attribution 4.0 International license. Further distribution of this work must maintain attribution to the author(s) and the published article's title, journal citation, and DOI. Funded by SCOAP[3].

 © 2026 CERN, for the LHCb Collaboration

TABLE I. Analyzed bins of dihadron mass for the (left) $K^+\pi^-$ and (right) K^+K^- final states.

Mass range (MeV/c^2)	
$792 < m_{K^+\pi^-} < 992$	$980 < m_{K^+K^-} < 1060$
$992 < m_{K^+\pi^-} < 1330$	$1060 < m_{K^+K^-} < 1200$
$1330 < m_{K^+\pi^-} < 1530$	$1200 < m_{K^+K^-} < 1400$
$1530 < m_{K^+\pi^-} < 1726$	$1400 < m_{K^+K^-} < 1600$
…	$1600 < m_{K^+K^-} < 1813$

The searches are conducted using a sample of pp collision data, corresponding to an integrated luminosity of 5.4 fb^{-1}, collected with the LHCb experiment during 2016–2018.

The dihadron invariant-mass spectra are split into bins to account for regions where the $K^+\pi^-$ and K^+K^- final states may be dominated by resonant or nonresonant contributions (see Table I). The range of dihadron masses investigated in the two searches spans from the low-mass resonances in each dihadron final state, K^{*0} and ϕ, for $K^+\pi^-$ and K^+K^-, respectively, up to their respective kinematic limits, $m_{B^0_{(s)}} - 2m_\tau$, where $m_{B^0_{(s)}}$ is the mass of the $B^0_{(s)}$ meson and m_τ is the mass of the tau lepton [40]. In order to avoid bias, the results of the analysis were not examined until the full procedure had been finalized.

The LHCb detector [41,42] is a single-arm forward spectrometer covering the pseudorapidity range $2 < \eta < 5$, designed for the study of particles containing b or c quarks. The detector elements that are particularly relevant to this analysis are: a silicon-strip vertex detector surrounding the pp interaction region that allows b and c hadrons to be identified from their characteristically long flight distance; a tracking system that provides a measurement of the momentum of charged particles; and two ring-imaging Cherenkov detectors that are able to discriminate between different species of charged hadrons. Muons are identified by a system composed of alternating layers of iron and multiwire proportional chambers. The online event selection, which is the same for both decays studied in this Letter, is performed by a hardware stage and two software stages [43]. The hardware stage requires events to have at least one muon with high transverse momentum. The software stages require a two-, three- or four-track secondary vertex with a significant displacement from all primary pp interaction vertices (PVs).

Simulation is used to model the effects of the detector acceptance and selection requirements on the signal decays and several specific background modes. In the simulation, pp collisions are generated using PYTHIA [44] with a specific LHCb configuration [45]. Decays of unstable particles are described by EVTGEN [46], in which final-state radiation is generated using PHOTOS [47]. The interaction of the generated particles with the detector and its response are implemented using the GEANT4 toolkit [48] as described in Ref. [49]. The simulated samples are weighted in order to account for known data-simulation differences in the $B^0_{(s)}$ production kinematics and detector occupancy, as well as hardware trigger efficiencies [50], track reconstruction efficiency [51] and particle-identification performance [52]. Each of these corrections is derived from dedicated control samples selected from the data.

The selection of signal candidates for each of the two final states follows the same strategy, although the precise requirements are not identical. Tracks are required to be of good quality, be displaced from any PV, meet minimum momentum requirements, and have particle-identification criteria consistent with the assigned particle hypotheses. The particle identification is particularly important in order to produce datasets for the two searches with minimal overlap.

Pairs of oppositely charged muons and hadrons are combined to form b-hadron candidates. The dihadron candidates are required to be consistent with originating from a common vertex, significantly separated from the associated PV, and to have a large momentum component transverse to the beam line. The associated PV is that which best aligns with the momentum vector of the (partially reconstructed) $B^0_{(s)}$ candidate. As the tau particles are expected to fly approximately in the direction of the b hadron, the vertex formed by the intersection of the two muon tracks is required to be located further downstream from the associated PV than the vertex formed by the intersection of the hadron tracks. In all two- and four-track combinations requirements are placed on the angle between the candidate momentum vector and the line of flight defined by the PV and candidate decay vertex.

Although different specific backgrounds are associated with each final state, the background categories and the strategies to reduce them are common between the two channels. A significant source of background consists of decays of the type $B^0_{(s)} \to D_s^-(\to h_1^+ h_2^- \mu^- \bar{\nu}_\mu)\mu^+\nu_\mu$, where $h_1^+ h_2^-$ represents either $K^+\pi^-$ or K^+K^- [40]. A criterion is imposed that the reconstructed $h_1^+ h_2^- \mu^-$ mass must be greater than the known D_s^- mass [40], which effectively rejects this background. While this reduces the signal efficiency by a factor of approximately 2, it reduces to negligible levels an otherwise irreducible set of large background modes.

Another significant background arises from decays of the type $B^0 \to D^{(*)}\bar{D}^{(*)}K^{*0}$ or $B_s^0 \to D^{(*)}\bar{D}^{(*)}\phi$, where both D mesons decay semimuonically. Selection requirements on the missing-mass squared, $m^2_{\rm miss}$, and the reconstructed q^2 reduce this background to a negligible level. The missing-mass squared is defined as $m^2_{\rm miss} = (P_{B^0_{(s)}} - P_{h_1^+h_2^-} - P_{\mu^+\mu^-})^2$, where $P_{B^0_{(s)}}$, $P_{h_1^+h_2^-}$, and $P_{\mu^+\mu^-}$ are the reconstructed four momenta of the b-hadron candidate, the dihadron pair, and the dimuon pair, respectively. The reconstructed q^2 is the square of the ditau invariant mass, estimated as $q^2 = (P_{B^0_{(s)}} - P_{h_1^+h_2^-})^2$. The $B^0_{(s)}$ four momentum cannot be determined precisely, as the $B^0_{(s)}$ candidate is partially

reconstructed. Therefore an approximation is used that assumes the proper velocity of the reconstructed $B^0_{(s)}$ candidate along the beam line is the true proper velocity [14]. The resulting estimated quantities have significant discriminating power, despite their limited resolution. This is due to the different decay topologies of the signal modes and the backgrounds. The particles producing the muons have different masses for signal ($\tau^+ \to \mu^+\nu_\mu\bar{\nu}_\tau$) and background ($D^+ \to \mu^+\nu_\mu X$, where X is any additional particle), resulting in different reconstructed q^2 distributions. In addition, the background decays contain fewer unreconstructed neutrinos (two) than signal (four) but can have additional neutral or charged particles such as K^0 mesons, and thus populate different regions of m^2_{miss}. Background modes such as $B^0 \to K^0_1\tau^+\tau^-$, where K^0_1 refers to $K_1(1270)^0$ and $K_1(1400)^0$ mesons, and $K^0_1 \to K^+\pi^-X$ (where X is any particle), have a negligible impact on this analysis given their small branching fractions.

After the selection requirements, the remaining components of the two datasets are in one of four categories: signal, either $B^0 \to K^+\pi^-\tau^+\tau^-$ or $B^0_s \to K^+K^-\tau^+\tau^-$; combinatorial background, which is formed from random combinations of tracks in the event; semileptonic cascade background, corresponding to decays of the type $B^0_{(s)} \to \bar{D}^0(\to h^+_1\mu^-\bar{\nu}_\mu)h^-_2\mu^+\nu_\mu$; and a small residual background from final-state particle misidentification. Multiclass boosted decision tree (BDT) [53,54] classifiers are trained to discriminate between signal, combinatorial background, and semileptonic cascade background. A separate BDT is optimized and trained for each final state and dihadron mass bin. The BDTs are implemented using the `lightgbm` package [55]. In training these BDTs, combinatorial background is represented with same-sign muon samples from the data, corresponding to the final state $h^+_1h^-_2\mu^+\mu^+$, as this sample is dominated by candidates formed from random combinations of tracks. The semileptonic cascade backgrounds are represented with simulated samples of the relevant decay modes. Signal is represented with simulated $B^0 \to K^+\pi^-\tau^+\tau^-$ and $B^0_s \to K^+K^-\tau^+\tau^-$ for the two dihadron modes that are investigated. In each case, the signal is generated uniformly in phase space.

A series of features pertaining to the separation of the muons from the dihadron vertex, as well as to the decay topology, are used to separate signal and background. The same features are used for the two searches and in each dihadron mass bin. Of particular importance are the reconstructed tau flight distance and a feature representing how well isolated the signal candidate is from other tracks in the event [56]. The tau flight distance is reconstructed with the assumption that the tau travels approximately in the direction of the b hadron, such that the intersection of the muon line of flight and b-hadron line of flight is an estimate of the tau decay vertex. Backgrounds with additional charged particles arise both from partially reconstructed decays of b hadrons, where one or more particles are not reconstructed, and from combinatorial background, in which tracks from several decays are wrongly identified as a candidate. In both cases, efficient reconstruction of the additional charged particles allows these backgrounds to be readily identified and rejected by a specific multivariate algorithm [56] which estimates the probability that an additional track in the event stems from the same vertex as the signal candidate.

The analysis sensitivity is affected by the hyperparameters of the BDTs, such as learning rate and maximum depth. Optimal values of these hyperparameters are determined for each final state and dihadron mass bin by maximizing a Punzi figure of merit [57] with the `optuna` [58] PYTHON package. The BDTs are trained using k-fold cross validation with the shapes of the output variables defined only from the test samples [59]. An early stopping procedure is used to avoid overtraining. After the selection procedure, less than 0.1% of remaining events have multiple candidates. In the cases where this happens, one candidate is arbitrarily selected per event. The efficiencies of the BDTs, given the preceding selections, vary between the bins because of the different kinematic distributions of the particles. In the dihadron mass bin including the K^{*0} resonance (corresponding to a $K^+\pi^-$ dihadron final state), the signal efficiency is 83%, while rejecting 95% of combinatorial background and 61% of semileptonic background for the maximal figure of merit. For the K^+K^- final state in the bin including the ϕ resonance, the maximal figure of merit is found where 87% of signal is kept for 92% combinatorial background and 42% semileptonic background rejection.

There is no suitable mass variable that can be fitted to determine the signal yields, due to the four unreconstructed neutrinos in the final state. An alternative strategy is therefore employed. Candidates are selected that have their BDT classifier score in the signal category higher than in either of the other categories. From these candidates, for each of the two searches, the signal yields in each dihadron mass bin are obtained from independent unbinned extended maximum-likelihood fits to the distribution of the BDT classifier output for the signal category. The shapes of each fit component are represented by Gaussian kernel density estimations (KDEs) [60]. Sigmoid functions are used to ensure that the distributions are exactly zero at the upper and lower edges of the BDT-output range. The BDT classifier output shapes are derived independently for each fit component and in each dihadron mass bin using either simulation or control samples. The optimal shape for each fit component is found by minimizing the likelihood of the relevant proxy sample as a function of the KDE bandwidth. The shapes for the signal modes and semileptonic cascade backgrounds are derived from simulation. The combinatorial shapes are established using the same-sign muon data control samples. Dedicated data control samples are used to unfold both the shape and the yield of the misidentified background components using the LHCb PIDCALIB package [61] and the

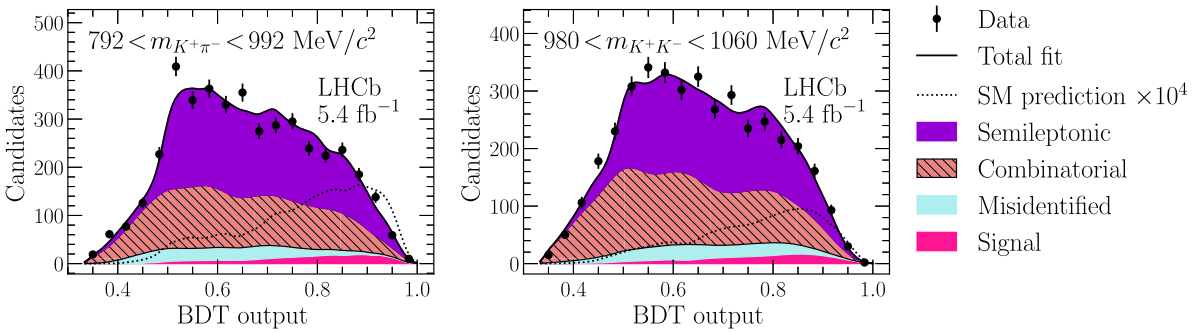

FIG. 1. Distribution of the BDT classifier output for selected candidates of the (left) $B^0 \to K^+\pi^-\tau^+\tau^-$ and (right) $B_s^0 \to K^+K^-\tau^+\tau^-$ data samples in the lowest dihadron mass bin of each. The respective fit results are also shown. The distribution for a hypothetical signal, with branching fraction enhanced by four orders of magnitude compared to the SM prediction, is also shown in each plot for illustrative purposes.

PYUNFOLD toolkit [62], as in Ref. [11]. The yields of all other fit components are floated.

For each of the two final states, the result of the fit to the lowest dihadron mass bin is shown in Fig. 1. As the signal yields are not significant in any bin, upper limits are set with the CL$_s$ method [63]. The fit quality for the background-only hypothesis is determined with pseudoexperiments and each bin is found to have a p-value in excess of 5%.

In order to obtain the upper limits on the signal branching fractions, the decays $B^0 \to J/\psi(\to \mu^+\mu^-)K^{*0}(\to K^+\pi^-)$ and $B_s^0 \to J/\psi(\to \mu^+\mu^-)\phi(\to K^+K^-)$ are used as separate normalization modes for the $B^0 \to K^+\pi^-\tau^+\tau^-$ and $B_s^0 \to K^+K^-\tau^+\tau^-$ searches, respectively. The branching fraction of one of the signal decays in a given dihadron mass bin i, $\mathcal{B}_i^{\rm sig}$ is calculated as

$$\mathcal{B}_i^{\rm sig} = \frac{N_i^{\rm sig}}{N^{\rm norm}} \times \frac{\epsilon^{\rm norm}}{\epsilon_i^{\rm sig}} \times \mathcal{B}^{\rm norm}, \tag{2}$$

where $N_i^{\rm sig}$ represents the signal yield in bin i and $\epsilon_i^{\rm sig}$ is the corresponding signal efficiency. The yield, efficiency, and branching fraction for the normalization mode are denoted by $N^{\rm norm}$, $\epsilon^{\rm norm}$, and $\mathcal{B}^{\rm norm}$, respectively. The efficiencies are derived from simulation. The normalization modes are chosen because their branching fractions are large and well established [40] and their reconstructed final states are identical to those of their respective signal modes.

The initial selection for the two normalization modes is the same as for the corresponding signal decays, but with the requirements on the reconstructed q^2 and $m^2_{\rm miss}$ omitted. Separate BDTs are trained for discriminating the normalization decays from backgrounds, with the same discriminating variables as for the BDTs used to select the signal candidates. However, as the normalization modes are fully reconstructed, backgrounds from partially reconstructed decays are minimal and so these BDTs discriminate only the normalization candidates from combinatorial background. The normalization yields are obtained from fits to the relevant $h_1^+h_2^-\mu^+\mu^-$ invariant-mass distributions.

The values of the extracted upper limits are impacted by systematic uncertainties. These are accounted for in the determination of the upper limits in the CL$_s$ method by variations of the models used to generate the pseudoexperiments. The most significant systematic uncertainty is due to the limited size of the data control samples used to construct the KDEs in the fits. These effects will be reduced with more data. The alternative models are made by resampling the proxy samples with replacement [64] to construct alternative KDEs.

The choice of KDE hyperparameters also affects the upper limit results. In order to model the effect of these choices, the pseudoexperiments used for the calculation of the upper limits with the CL$_s$ method are generated varying the bandwidths within two standard deviations of their optimal value, both with and without sigmoid functions.

A further source of uncertainty arises from the phase-space model used to simulate the two signal decay modes. Weights are applied to emulate alternative physics models, using predictions from Refs. [65–72] implemented with the FLAVIO [73] package. The changes in BDT output shapes and in the overall signal efficiencies are minimal when physics models with $\mathcal{O}(10^2)$ shifts in the Wilson coefficients $\mathcal{C}_9^{\tau\tau}$ and $\mathcal{C}_{10}^{\tau\tau}$ are taken into account, and when incorporating uncertainties due to the simulation corrections.

The analysis method is validated by analyzing several decay modes with the same final states as the signals under study. The branching fractions of $B_s^0 \to K^+K^-\mu^+\mu^-$ and $B^0 \to K^+\pi^-\mu^+\mu^-$ are obtained with the fits of an appropriate BDT classifier score and compared to previous measurements [3,5]. The results extracted with this method are found to be consistent with the published numbers.

The resulting CL$_s$ upper limits for $B^0 \to K^+\pi^-\tau^+\tau^-$ and $B_s^0 \to K^+K^-\tau^+\tau^-$ in each of the dihadron mass bins are given in Table II, and the CL$_s$ scans for the lightest dihadron mass bins are shown in Fig. 2. The $B^0 \to K^+\pi^-\tau^+\tau^-$ results

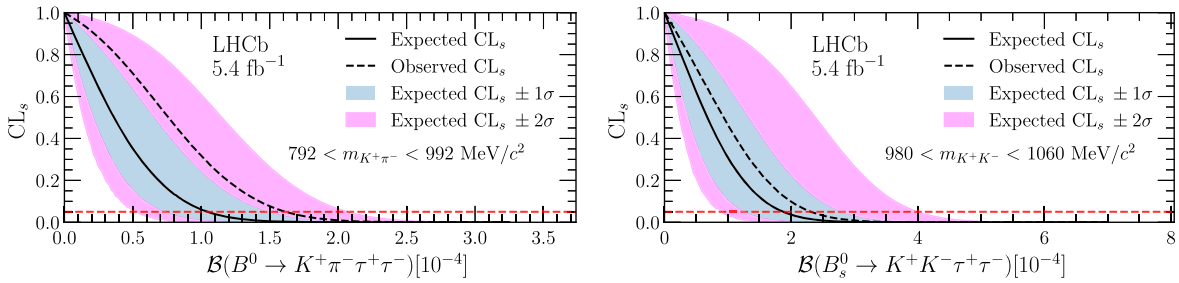

FIG. 2. Expected and observed upper limits obtained with the CL$_s$ method for the lightest bins containing (left) $K^+\pi^-$ and (right) K^+K^- final states.

are recast as a search for the decay $B_s^0 \to K^-\pi^+\tau^+\tau^-$, which proceeds via a $b \to d\tau^+\tau^-$ transition, using the ratio of hadronization fractions (f_s/f_d) [74]. The resulting upper limits are also given in Table II and are the first for this process.

The upper limit for the $B^0 \to K^+\pi^-\tau^+\tau^-$ decay in the $792 < m_{K^+\pi^-} < 992$ MeV/c^2 bin is reinterpreted as a limit on the $B^0 \to K^{*0}\tau^+\tau^-$ decay by assuming that the K^{*0} resonance is the only contribution, and accounting for the $K^{*0} \to K^+\pi^-$ branching fraction [40] and the fraction of the K^{*0} resonance that lies within this mass range. Similarly, the $B_s^0 \to K^+K^-\tau^+\tau^-$ search in the $980 < m_{K^+K^-} < 1060$ MeV/c^2 bin is reinterpreted as a search for the decay $B_s^0 \to \phi\tau^+\tau^-$. The results of these reinterpretations are

$$\mathcal{B}(B^0 \to K^{*0}\tau^+\tau^-) < 2.8 \times 10^{-4}(2.5 \times 10^{-4}) \text{ at } 95\%(90\%)\,\text{CL},$$
$$\mathcal{B}(B_s^0 \to \phi\tau^+\tau^-) < 4.7 \times 10^{-4}(4.1 \times 10^{-4}) \text{ at } 95\%(90\%)\,\text{CL}.$$

Combining these upper limits and the model and assumptions from Ref. [27], limits are also set on the square of the shift Δ in the Wilson coefficients $\mathcal{C}_9^{\tau\tau}$ and $\mathcal{C}_{10}^{\tau\tau}$, defined in Eq. (1). The resulting upper limits are shown in Table III. These are tighter constraints than those obtained in Ref. [8] by more than a factor of 3.

In summary, this Letter reports searches for the $b \to s\tau^+\tau^-$ decays $B^0 \to K^+\pi^-\tau^+\tau^-$ and $B_s^0 \to K^+K^-\tau^+\tau^-$. No significant signal is observed for either decay and upper limits on the respective branching fractions are set. Interpreting the former as a search for the $B^0 \to K^{*0}\tau^+\tau^-$ decay leads to an upper limit on the branching fraction of this decay that is an order of magnitude better than the current world's best [37]. The searches for the B_s^0 decay mode are the world's first. Given the anomalies observed in the measurements of $R(D^{(*)})$, a range of new physics models have been constructed that predict significant enhancements in the branching fractions of these decay modes. This analysis augurs a comprehensive program of $b \to s\tau^+\tau^-$ searches at LHCb that will challenge such new-physics models with the data collected in the ongoing Large Hadron Collider run.

TABLE II. Upper limits on the branching fractions of $B^0 \to K^+\pi^-\tau^+\tau^-$, $B_s^0 \to K^+K^-\tau^+\tau^-$, and $B_s^0 \to K^-\pi^+\tau^+\tau^-$ decays in the analyzed bins of dihadron mass at 90% and 95% CL.

Confidence level	Upper limit on $\mathcal{B}(B^0 \to K^+\pi^-\tau^+\tau^-)$			
$m_{K^+\pi^-}$ (MeV/c^2)	[792, 992]	[992, 1330]	[1330, 1530]	[1530, 1726]
90%	1.4×10^{-4}	2.7×10^{-5}	1.0×10^{-5}	2.7×10^{-6}
95%	1.6×10^{-4}	3.4×10^{-5}	1.1×10^{-5}	3.3×10^{-6}

Confidence level	Upper limit on $\mathcal{B}(B_s^0 \to K^+K^-\tau^+\tau^-)$				
$m_{K^+K^-}$ (MeV/c^2)	[980, 1060]	[1060, 1200]	[1200, 1400]	[1400, 1600]	[1600, 1813]
90%	2.0×10^{-4}	1.3×10^{-4}	1.2×10^{-4}	6.8×10^{-5}	3.2×10^{-5}
95%	2.3×10^{-4}	1.5×10^{-4}	1.4×10^{-4}	7.6×10^{-5}	3.6×10^{-5}

Confidence level	Upper limit on $\mathcal{B}(B_s^0 \to K^-\pi^+\tau^+\tau^-)$			
$m_{K^+\pi^-}$ (MeV/c^2)	[792, 992]	[992, 1330]	[1330, 1530]	[1530, 1726]
90%	6.5×10^{-4}	1.2×10^{-4}	5.1×10^{-5}	1.7×10^{-5}
95%	7.3×10^{-4}	1.5×10^{-4}	6.2×10^{-5}	2.1×10^{-5}

TABLE III. Upper limit on Δ^2 at 90% and 95% CL.

Confidence level	$B^0 \to K^+\pi^-\tau^+\tau^-$	$B_s^0 \to K^+K^-\tau^+\tau^-$
90%	2.5×10^4	4.5×10^4
95%	2.9×10^4	5.2×10^4

Acknowledgments—We express our gratitude to our colleagues in the CERN accelerator departments for the excellent performance of the LHC. We thank the technical and administrative staff at the LHCb institutes. We acknowledge support from CERN and from the national agencies: ARC (Australia); CAPES, CNPq, FAPERJ, and FINEP (Brazil); MOST and NSFC (China); CNRS/IN2P3 (France); BMFTR, DFG, and MPG (Germany); INFN (Italy); NWO (Netherlands); MNiSW and NCN (Poland); MCID/IFA (Romania); MICIU and AEI (Spain); SNSF and SER (Switzerland); NASU (Ukraine); STFC (United Kingdom); DOE NP and NSF (USA). We acknowledge the computing resources that are provided by ARDC (Australia), CBPF (Brazil), CERN, IHEP, and LZU (China), IN2P3 (France), KIT and DESY (Germany), INFN (Italy), SURF (Netherlands), Polish WLCG (Poland), IFIN-HH (Romania), PIC (Spain), CSCS (Switzerland), and GridPP (United Kingdom). We are indebted to the communities behind the multiple open-source software packages on which we depend. Individual groups or members have received support from Key Research Program of Frontier Sciences of CAS, CAS PIFI, CAS CCEPP, Fundamental Research Funds for the Central Universities, and Sci. & Tech. Program of Guangzhou (China); Minciencias (Colombia); EPLANET, Marie Skłodowska-Curie Actions, ERC and NextGenerationEU (European Union); A*MIDEX, ANR, IPhU and Labex P2IO, and Région Auvergne-Rhône-Alpes (France); Alexander-von-Humboldt Foundation (Germany); ICSC (Italy); Severo Ochoa and María de Maeztu Units of Excellence, GVA, XuntaGal, GENCAT, InTalent-Inditex and Prog. Atracción Talento CM (Spain); SRC (Sweden); the Leverhulme Trust, the Royal Society and UKRI (United Kingdom).

Data availability—Data associated with the plots in this publication are made available on the CERN Document Server in Ref. [75].

[1] R. Aaij *et al.* (LHCb Collaboration), Differential branching fractions and isospin asymmetries of $B \to K^{(*)}\mu^+\mu^-$ decays, J. High Energy Phys. 06 (2014) 133.

[2] R. Aaij *et al.* (LHCb Collaboration), Differential branching fraction and angular moments analysis of the decay $B^0 \to K^+\pi^-\mu^+\mu^-$ in the $K^*_{0,2}(1430)^0$ region, J. High Energy Phys. 12 (2016) 065.

[3] R. Aaij *et al.* (LHCb Collaboration), Measurements of the S-wave fraction in $B^0 \to K^+\pi^-\mu^+\mu^-$ decays and the $B^0 \to K^*(892)^0\mu^+\mu^-$ differential branching fraction, J. High Energy Phys. 11 (2016) 047; 04 (2017) 142(E).

[4] R. Aaij *et al.* (LHCb Collaboration), Measurement of *CP*-averaged observables in the $B^0 \to K^{*0}\mu^+\mu^-$ decay, Phys. Rev. Lett. **125**, 011802 (2020).

[5] R. Aaij *et al.* (LHCb Collaboration), Branching fraction measurements of the rare $B_s^0 \to \phi\mu^+\mu^-$ and $B_s^0 \to f_2'(1525)\mu^+\mu^-$ decays, Phys. Rev. Lett. **127**, 151801 (2021).

[6] R. Aaij *et al.* (LHCb Collaboration), Determination of short- and long-distance contributions in $B^0 \to K^{*0}\mu^+\mu^-$ decays, Phys. Rev. D **109**, 052009 (2024).

[7] R. Aaij *et al.* (LHCb Collaboration), Amplitude analysis of the $B^0 \to K^{*0}\mu^+\mu^-$ decay, Phys. Rev. Lett. **132**, 131801 (2024).

[8] R. Aaij *et al.* (LHCb Collaboration), Comprehensive analysis of local and nonlocal amplitudes in the $B^0 \to K^{*0}\mu^+\mu^-$ decay, J. High Energy Phys. 09 (2024) 026; 05 (2025) 208 (E).

[9] A. Hayrapetyan *et al.* (CMS Collaboration), Angular analysis of the $B^0 \to K^*(892)^0\mu^+\mu^-$ decay in proton-proton collisions at $\sqrt{s} = 13$ TeV, Phys. Lett. B **864**, 139406 (2025).

[10] S. Wehle *et al.* (Belle Collaboration), Lepton-flavor-dependent angular analysis of $B \to K^*\ell^+\ell^-$, Phys. Rev. Lett. **118**, 111801 (2017).

[11] R. Aaij *et al.* (LHCb Collaboration), Measurement of the branching fraction ratios $R(D^+)$ and $R(D^{*+})$ using muonic τ decays, Phys. Rev. Lett. **134**, 061801 (2025).

[12] R. Aaij *et al.* (LHCb Collaboration), Test of lepton flavor universality by the measurement of the $B^0 \to D^{*-}\tau^+\nu_\tau$ branching fraction using three-prong τ decays, Phys. Rev. D **97**, 072013 (2018).

[13] R. Aaij *et al.* (LHCb Collaboration), Measurement of the ratio of the $\mathcal{B}(B^0 \to D^{*-}\tau^+\nu_\tau)$ and $\mathcal{B}(B^0 \to D^{*-}\mu^+\nu_\mu)$ branching fractions using three-prong τ-lepton decays, Phys. Rev. Lett. **120**, 171802 (2018).

[14] R. Aaij *et al.* (LHCb Collaboration), Measurement of the ratio of branching fractions $\mathcal{B}(\bar{B}^0 \to D^{*+}\tau^-\bar{\nu}_\tau)/\mathcal{B}(\bar{B}^0 \to D^{*+}\mu^-\bar{\nu}_\mu)$, Phys. Rev. Lett. **115**, 111803 (2015); **115**, 159901 (2015).

[15] R. Aaij *et al.* (LHCb Collaboration), Measurement of the ratio of branching fractions $\mathcal{R}(D^*)$ and $\mathcal{R}(D^0)$, Phys. Rev. Lett. **131**, 111802 (2023).

[16] J. P. Lees *et al.* (*BABAR* Collaboration), Evidence for an excess of $\bar{B} \to D^{(*)}\tau^-\bar{\nu}_\tau$ decays, Phys. Rev. Lett. **109**, 101802 (2012).

[17] M. Huschle *et al.* (Belle Collaboration), Measurement of the branching ratio of $\bar{B} \to D^{(*)}\tau^-\bar{\nu}_\tau$ relative to $\bar{B} \to D^{(*)}\ell^-\bar{\nu}_\ell$ decays with hadronic tagging at Belle, Phys. Rev. D **92**, 072014 (2015).

[18] S. Hirose *et al.* (Belle Collaboration), Measurement of the τ lepton polarization and $R(D^*)$ in the decay $\bar{B} \to D^*\tau^-\bar{\nu}_\tau$ with one-prong hadronic τ decays at Belle, Phys. Rev. D **97**, 012004 (2018).

[19] G. Caria *et al.* (Belle Collaboration), Measurement of $\mathcal{R}(D)$ and $\mathcal{R}(D^*)$ with a semileptonic tagging method, Phys. Rev. Lett. **124**, 161803 (2020).

[20] I. Adachi *et al.* (Belle II Collaboration), First measurement of $R(X_{\tau/\ell})$ as an inclusive test of the $b \to c\tau\nu$ anomaly, Phys. Rev. Lett. **132**, 211804 (2024).

[21] I. Adachi *et al.* (Belle II Collaboration), Test of lepton flavor universality with a measurement of $R(D^*)$ using hadronic B tagging at the Belle II experiment, Phys. Rev. D **110**, 072020 (2024).

[22] I. Adachi *et al.* (Belle II Collaboration), Test of lepton flavor universality with measurements of $R(D^+)$ and $R(D^{*+})$ using semileptonic B tagging at the Belle II experiment, Phys. Rev. D **112**, 032010 (2025).

[23] R. Alonso, B. Grinstein, and J. Martin Camalich, Lepton universality violation and lepton flavor conservation in B-meson decays, J. High Energy Phys. 10 (2015) 184.

[24] R. Barbieri, G. Isidori, A. Pattori, and F. Senia, Anomalies in B-decays and $U(2)$ flavour symmetry, Eur. Phys. J. C **76**, 67 (2016).

[25] A. Crivellin, D. Müller, and T. Ota, Simultaneous explanation of $R(D^{(*)})$ and $b \to s\mu^+\mu^-$: The last scalar leptoquarks standing, J. High Energy Phys. 09 (2017) 040.

[26] D. Buttazzo, A. Greljo, G. Isidori, and D. Marzocca, B-physics anomalies: A guide to combined explanations, J. High Energy Phys. 11 (2017) 044.

[27] B. Capdevila *et al.*, Searching for new physics with $b \to s\tau^+\tau^-$ processes, Phys. Rev. Lett. **120**, 181802 (2018).

[28] M. Bordone, C. Cornella, J. Fuentes-Martín, and G. Isidori, Low-energy signatures of the PS^3 model: From B-physics anomalies to LFV, J. High Energy Phys. 10 (2018) 148.

[29] W. Altmannshofer, P. S. Bhupal Dev, A. Soni, and Y. Sui, Addressing $R_{D^{(*)}}$, $R_{K^{(*)}}$, muon $g-2$ and ANITA anomalies in a minimal R-parity violating supersymmetric framework, Phys. Rev. D **102**, 015031 (2020).

[30] J. Aebischer *et al.*, Confronting the vector leptoquark hypothesis with new low- and high-energy data, Eur. Phys. J. C **83**, 153 (2023).

[31] A. Crivellin, D. Müller, and F. Saturnino, Flavor phenomenology of the leptoquark singlet-triplet model, J. High Energy Phys. 06 (2020) 020.

[32] M. Algueró, J. Matias, B. Capdevila, and A. Crivellin, Disentangling lepton flavor universal and lepton flavor universality violating effects in $b \to s\ell^+\ell^-$ transitions, Phys. Rev. D **105**, 113007 (2022).

[33] C. Bobeth and U. Haisch, New physics in Γ_{12}^s: $(\bar{s}b)(\bar{\tau}\tau)$ operators, Acta Phys. Pol. B **44**, 127 (2013).

[34] R. Aaij *et al.* (LHCb Collaboration), Search for the decays $B_s^0 \to \tau^+\tau^-$ and $B^0 \to \tau^+\tau^-$, Phys. Rev. Lett. **118**, 251802 (2017).

[35] J. P. Lees *et al.* (*BABAR* Collaboration), Search for $B^+ \to K^+\tau^+\tau^-$ at the *BABAR* experiment, Phys. Rev. Lett. **118**, 031802 (2017).

[36] T. V. Dong *et al.* (Belle Collaboration), Search for the decay $B^0 \to K^{*0}\tau^+\tau^-$ at the Belle experiment, Phys. Rev. D **108**, L011102 (2023).

[37] I. Adachi *et al.* (Belle II Collaboration), Search for $B^0 \to K^{*0}\tau^+\tau^-$ decays at the Belle II experiment, Phys. Rev. Lett. **135**, 151801 (2025).

[38] C. Cornella *et al.*, Hunting for $B^+ \to K^+\tau^+\tau^-$ imprints on the $B^+ \to K^+\mu^+\mu^-$ dimuon spectrum, Eur. Phys. J. C **80**, 1095 (2020).

[39] F. Archilli *et al.*, Performance of the muon identification at LHCb, J. Instrum. **8**, P10020 (2013).

[40] S. Navas *et al.* (Particle Data Group), Review of particle physics, Phys. Rev. D **110**, 030001 (2024).

[41] A. A. Alves Jr. *et al.* (LHCb Collaboration), The LHCb detector at the LHC, J. Instrum. **3**, S08005 (2008).

[42] R. Aaij *et al.* (LHCb Collaboration), LHCb detector performance, Int. J. Mod. Phys. A **30**, 1530022 (2015).

[43] R. Aaij *et al.*, Design and performance of the LHCb trigger and full real-time reconstruction in Run 2 of the LHC, J. Instrum. **14**, P04013 (2019).

[44] T. Sjöstrand, S. Mrenna, and P. Skands, A brief introduction to PYTHIA8.1, Comput. Phys. Commun. **178**, 852 (2008).

[45] I. Belyaev *et al.*, Handling of the generation of primary events in Gauss, the LHCb simulation framework, J. Phys. Conf. Ser. **331**, 032047 (2011).

[46] D. J. Lange, The EVTGEN particle decay simulation package, Nucl. Instrum. Methods Phys. Res., Sect. A **462**, 152 (2001).

[47] N. Davidson, T. Przedzinski, and Z. Was, PHOTOS interface in C++: Technical and physics documentation, Comput. Phys. Commun. **199**, 86 (2016).

[48] J. Allison *et al.* (GEANT4 Collaboration), GEANT4 developments and applications, IEEE Trans. Nucl. Sci. **53**, 270 (2006); S. Agostinelli *et al.* (GEANT4 Collaboration), GEANT4: A simulation toolkit, Nucl. Instrum. Methods Phys. Res., Sect. A **506**, 250 (2003).

[49] M. Clemencic *et al.*, The LHCb simulation application, Gauss: Design, evolution and experience, J. Phys. Conf. Ser. **331**, 032023 (2011).

[50] S. Tolk, J. Albrecht, F. Dettori, and A. Pellegrino, Data driven trigger efficiency determination at LHCb, CERN, LHCb-PUB-2014-039, 2014.

[51] R. Aaij *et al.* (LHCb Collaboration), Measurement of the track reconstruction efficiency at LHCb, J. Instrum. **10**, P02007 (2015).

[52] L. Anderlini *et al.*, The PIDCALIB package, CERN, LHCb-PUB-2016-021, 2016.

[53] L. Breiman, J. H. Friedman, R. A. Olshen, and C. J. Stone, *Classification and Regression Trees* (Wadsworth International Group, Belmont, California, USA, 1984).

[54] Y. Freund and R. E. Schapire, A decision-theoretic generalization of on-line learning and an application to boosting, J. Comput. Syst. Sci. **55**, 119 (1997).

[55] G. Ke *et al.*, LightGBM: A highly efficient gradient boosting decision tree, in *Advances in Neural Information Processing Systems*, edited by I. Guyon *et al.* (Curran Associates, Inc., Red Hook, NY, 2017), 30.

[56] R. Aaij *et al.* (LHCb Collaboration), Determination of the quark coupling strength $|V_{ub}|$ using baryonic decays, Nat. Phys. **11**, 743 (2015).

[57] G. Punzi, Sensitivity of searches for new signals and its optimization, eConf C **030908**, MODT002 (2003).

[58] T. Akiba *et al.*, Optuna: A next-generation hyperparameter optimization framework, in *Proceedings of the 25th ACM SIGKDD International Conference on Knowledge Discovery and Data Mining* (2019), arXiv:1907.10902.

[59] A. Blum, A. Kalai, and J. Langford, Beating the hold-out: Bounds for K-fold and progressive cross-validation, in *Proceedings of the Twelfth Annual Conference on Computational Learning Theory (COLT '99): Santa Cruz, California, USA, 1999* (Wadsworth International Group, Belmont, 1999), 203.

[60] K. S. Cranmer, Kernel estimation in high-energy physics, Comput. Phys. Commun. **136**, 198 (2001).
[61] R. Aaij *et al.*, Selection and processing of calibration samples to measure the particle identification performance of the LHCb experiment in Run 2, Eur. Phys. J. Tech. Instrum. **6**, 1 (2019).
[62] J. Bourbeau and Z. Hampel-Arias, PYUNFOLD: A PYTHON package for iterative unfolding, J. Open Source Software **3**, 741 (2018).
[63] A. L. Read, Presentation of search results: The CL_s technique, J. Phys. G **28**, 2693 (2002).
[64] B. Efron, Bootstrap methods: Another look at the jackknife, Ann. Stat. **7**, 1 (1979).
[65] D. Seidel, Analytic two loop virtual corrections to $b \to d\ell^+\ell^-$, Phys. Rev. D **70**, 094038 (2004).
[66] M. Beneke, G. Buchalla, A. Lenz, and U. Nierste, *CP* Asymmetry in flavor specific B decays beyond leading logarithms, Phys. Lett. B **576**, 173 (2003).
[67] S. Descotes-Genon and J. Virto, Time dependence in $B \to V\ell\ell$ decays, J. High Energy Phys. 04 (2015) 045; 07 (2015) 049.
[68] T. Inami and C. S. Lim, Effects of superheavy quarks and leptons in low-energy weak processes $K_L \to \mu\bar{\mu}$, $K^+ \to \pi^+\nu\bar{\nu}$ and $K^0 \leftrightarrow \bar{K}^0$, Prog. Theor. Phys. **65**, 297 (1981); **65**, 1772(E) (1981).
[69] M. Beneke, T. Feldmann, and D. Seidel, Exclusive radiative and electroweak $b \to d$ and $b \to s$ penguin decays at NLO, Eur. Phys. J. C **41**, 173 (2005).
[70] H. M. Asatrian, K. Bieri, C. Greub, and M. Walker, Virtual corrections and bremsstrahlung corrections to $b \to d\ell^+\ell^-$ in the standard model, Phys. Rev. D **69**, 074007 (2004).
[71] A. Bharucha, D. M. Straub, and R. Zwicky, $B \to V\ell^+\ell^-$ in the standard model from light-cone sum rules, J. High Energy Phys. 08 (2016) 098.
[72] C. Bobeth *et al.*, $B_{s,d} \to \ell^+\ell^-$ in the standard model with reduced theoretical uncertainty, Phys. Rev. Lett. **112**, 101801 (2014).
[73] D. M. Straub, FLAVIO: A PYTHON package for flavour and precision phenomenology in the standard model and beyond, arXiv:1810.08132.
[74] R. Aaij *et al.* (LHCb Collaboration), Precise measurement of the f_s/f_d ratio of fragmentation fractions and of B^0_s decay branching fractions, Phys. Rev. D **104**, 032005 (2021).
[75] https://cds.cern.ch/record/2946087.

R. Aaij,[38] A. S. W. Abdelmotteleb,[58] C. Abellan Beteta,[52] F. Abudinén,[58] T. Ackernley,[62] A. A. Adefisoye,[70] B. Adeva,[48] M. Adinolfi,[56] P. Adlarson,[86] C. Agapopoulou,[14] C. A. Aidala,[88] Z. Ajaltouni,[11] S. Akar,[11] K. Akiba,[38] M. Akthar,[40] P. Albicocco,[28] J. Albrecht,[19,b] R. Aleksiejunas,[82] F. Alessio,[50] P. Alvarez Cartelle,[57,48] R. Amalric,[16] S. Amato,[3] J. L. Amey,[56] Y. Amhis,[14] L. An,[6] L. Anderlini,[27] M. Andersson,[52] P. Andreola,[52] M. Andreotti,[26] S. Andres Estrada,[45] A. Anelli,[31,50,c] D. Ao,[7] C. Arata,[12] F. Archilli,[37,d] Z. Areg,[70] M. Argenton,[26] S. Arguedas Cuendis,[9,50] L. Arnone,[31,c] A. Artamonov,[44] M. Artuso,[70] E. Aslanides,[13] R. Ataíde Da Silva,[51] M. Atzeni,[66] B. Audurier,[12] J. A. Authier,[15] D. Bacher,[65] I. Bachiller Perea,[51] S. Bachmann,[22] M. Bachmayer,[51] J. J. Back,[58] P. Baladron Rodriguez,[48] V. Balagura,[15] A. Balboni,[26] W. Baldini,[26] Z. Baldwin,[80] L. Balzani,[19] H. Bao,[7] J. Baptista de Souza Leite,[2] C. Barbero Pretel,[48,12] M. Barbetti,[27] I. R. Barbosa,[71] R. J. Barlow,[64,a] M. Barnyakov,[25] S. Barsuk,[14] W. Barter,[60] J. Bartz,[70] S. Bashir,[40] B. Batsukh,[5] P. B. Battista,[14] A. Bay,[51] A. Beck,[66] M. Becker,[19] F. Bedeschi,[35] I. B. Bediaga,[2] N. A. Behling,[19] S. Belin,[48] A. Bellavista,[25] K. Belous,[44] I. Belov,[29] I. Belyaev,[36] G. Benane,[13] G. Bencivenni,[28] E. Ben-Haim,[16] A. Berezhnoy,[44] R. Bernet,[52] S. Bernet Andres,[47] A. Bertolin,[33] F. Betti,[60] J. Bex,[57] O. Bezshyyko,[87] S. Bhattacharya,[81] J. Bhom,[41] M. S. Bieker,[18] N. V. Biesuz,[26] A. Biolchini,[38] M. Birch,[63] F. C. R. Bishop,[10] A. Bitadze,[64] A. Bizzeti,[27,e] T. Blake,[58,f] F. Blanc,[51] J. E. Blank,[19] S. Blusk,[70] V. Bocharnikov,[44] J. A. Boelhauve,[19] O. Boente Garcia,[50] T. Boettcher,[69] A. Bohare,[60] A. Boldyrev,[44] C. S. Bolognani,[84] R. Bolzonella,[26,g] R. B. Bonacci,[1] N. Bondar,[44,50] A. Bordelius,[50] F. Borgato,[33,50] S. Borghi,[64] M. Borsato,[31,c] J. T. Borsuk,[85] E. Bottalico,[62] S. A. Bouchiba,[51] M. Bovill,[65] T. J. V. Bowcock,[62] A. Boyer,[50] C. Bozzi,[26] J. D. Brandenburg,[89] A. Brea Rodriguez,[51] N. Breer,[19] J. Brodzicka,[41] J. Brown,[62] D. Brundu,[32] E. Buchanan,[60] M. Burgos Marcos,[84] A. T. Burke,[64] C. Burr,[50] C. Buti,[27] J. S. Butter,[57] J. Buytaert,[50] W. Byczynski,[50] S. Cadeddu,[32] H. Cai,[76] Y. Cai,[5] A. Caillet,[16] R. Calabrese,[26,g] S. Calderon Ramirez,[9] L. Calefice,[46] M. Calvi,[31,c] M. Calvo Gomez,[47] P. Camargo Magalhaes,[2,h] J. I. Cambon Bouzas,[48] P. Campana,[28] A. F. Campoverde Quezada,[7] S. Capelli,[31] M. Caporale,[25] L. Capriotti,[26] R. Caravaca-Mora,[9] A. Carbone,[25,i] L. Carcedo Salgado,[48] R. Cardinale,[29,j] A. Cardini,[32] P. Carniti,[31] L. Carus,[22] A. Casais Vidal,[66] R. Caspary,[22] G. Casse,[62] M. Cattaneo,[50] G. Cavallero,[26] V. Cavallini,[26,g] S. Celani,[50] I. Celestino,[35,k] S. Cesare,[30,l] A. J. Chadwick,[62] I. Chahrour,[88] H. Chang,[4,m] M. Charles,[16] Ph. Charpentier,[50] E. Chatzianagnostou,[38] R. Cheaib,[81] M. Chefdeville,[10]

C. Chen,[57] J. Chen,[51] S. Chen,[5] Z. Chen,[7] A. Chen Hu,[63] M. Cherif,[12] A. Chernov,[41] S. Chernyshenko,[54] X. Chiotopoulos,[84] V. Chobanova,[45] M. Chrzaszcz,[41] A. Chubykin,[44] V. Chulikov,[28,36,50] P. Ciambrone,[28] X. Cid Vidal,[48] G. Ciezarek,[50] P. Cifra,[38] P. E. L. Clarke,[60] M. Clemencic,[50] H. V. Cliff,[57] J. Closier,[50] C. Cocha Toapaxi,[22] V. Coco,[50] J. Cogan,[13] E. Cogneras,[11] L. Cojocariu,[43] S. Collaviti,[51] P. Collins,[50] T. Colombo,[50] M. Colonna,[19] A. Comerma-Montells,[46] L. Congedo,[24] J. Connaughton,[58] A. Contu,[32] N. Cooke,[61] G. Cordova,[35,k] C. Coronel,[67] I. Corredoira,[12] A. Correia,[16] G. Corti,[50] J. Cottee Meldrum,[56] B. Couturier,[50] D. C. Craik,[52] M. Cruz Torres,[2,n] M. Cubero Campos,[9] E. Curras Rivera,[51] R. Currie,[60] C. L. Da Silva,[69] S. Dadabaev,[44] X. Dai,[4] E. Dall'Occo,[50] J. Dalseno,[45] C. D'Ambrosio,[63] J. Daniel,[11] G. Darze,[3] A. Davidson,[58] J. E. Davies,[64] O. De Aguiar Francisco,[64] C. De Angelis,[32,o] F. De Benedetti,[50] J. de Boer,[38] K. De Bruyn,[83] S. De Capua,[64] M. De Cian,[64,50] U. De Freitas Carneiro Da Graca,[2,p] E. De Lucia,[28] J. M. De Miranda,[2] L. De Paula,[3] M. De Serio,[24,q] P. De Simone,[28] F. De Vellis,[19] J. A. de Vries,[84] F. Debernardis,[24] D. Decamp,[10] S. Dekkers,[1] L. Del Buono,[16] B. Delaney,[66] H.-P. Dembinski,[19] J. Deng,[8] V. Denysenko,[52] O. Deschamps,[11] F. Dettori,[32,o] B. Dey,[81] P. Di Nezza,[28] I. Diachkov,[44] S. Didenko,[44] S. Ding,[70] Y. Ding,[51] L. Dittmann,[22] V. Dobishuk,[54] A. D. Docheva,[61] A. Doheny,[58] C. Dong,[4,m] A. M. Donohoe,[23] F. Dordei,[32] A. C. dos Reis,[2] A. D. Dowling,[70] L. Dreyfus,[13] W. Duan,[74] P. Duda,[85] L. Dufour,[50] V. Duk,[34] P. Durante,[50] M. M. Duras,[85] J. M. Durham,[69] O. D. Durmus,[81] A. Dziurda,[41] A. Dzyuba,[44] S. Easo,[59] E. Eckstein,[18] U. Egede,[1] A. Egorychev,[44] V. Egorychev,[44] S. Eisenhardt,[60] E. Ejopu,[62] L. Eklund,[86] M. Elashri,[67] D. Elizondo Blanco,[9] J. Ellbracht,[19] S. Ely,[63] A. Ene,[43] J. Eschle,[70] S. Esen,[22] T. Evans,[38] F. Fabiano,[32] S. Faghih,[67] L. N. Falcao,[31,c] B. Fang,[7] R. Fantechi,[35] L. Fantini,[34,r] M. Faria,[51] K. Farmer,[60] F. Fassin,[83,38] D. Fazzini,[31,c] L. Felkowski,[85] M. Feng,[5,7] A. Fernandez Casani,[49] M. Fernandez Gomez,[48] A. D. Fernez,[68] F. Ferrari,[25,i] F. Ferreira Rodrigues,[3] M. Ferrillo,[52] M. Ferro-Luzzi,[50] S. Filippov,[44] R. A. Fini,[24] M. Fiorini,[26,g] M. Firlej,[40] K. L. Fischer,[65] D. S. Fitzgerald,[88] C. Fitzpatrick,[64] T. Fiutowski,[40] F. Fleuret,[15] A. Fomin,[53] M. Fontana,[25] L. A. Foreman,[64] R. Forty,[50] D. Foulds-Holt,[60] V. Franco Lima,[3] M. Franco Sevilla,[68] M. Frank,[50] E. Franzoso,[26,g] G. Frau,[64] C. Frei,[50] D. A. Friday,[64,50] J. Fu,[7] Q. Führing,[19,57,b] T. Fulghesu,[13] G. Galati,[24,q] M. D. Galati,[38] A. Gallas Torreira,[48] D. Galli,[25,i] S. Gambetta,[60] M. Gandelman,[3] P. Gandini,[30] B. Ganie,[64] H. Gao,[7] R. Gao,[65] T. Q. Gao,[57] Y. Gao,[8] Y. Gao,[6] Y. Gao,[8] L. M. Garcia Martin,[51] P. Garcia Moreno,[46] J. García Pardiñas,[66] P. Gardner,[68] L. Garrido,[46] C. Gaspar,[50] A. Gavrikov,[33] L. L. Gerken,[19] E. Gersabeck,[20] M. Gersabeck,[20] T. Gershon,[58] S. Ghizzo,[29,j] Z. Ghorbanimoghaddam,[56] F. I. Giasemis,[16,s] V. Gibson,[57] H. K. Giemza,[42] A. L. Gilman,[67] M. Giovannetti,[28] A. Gioventù,[46] L. Girardey,[64,59] M. A. Giza,[41] F. C. Glaser,[14,22] V. V. Gligorov,[16] C. Göbel,[71] L. Golinka-Bezshyyko,[87] E. Golobardes,[47] D. Golubkov,[44] A. Golutvin,[63,50] S. Gomez Fernandez,[46] W. Gomulka,[40] I. Gonçales Vaz,[50] F. Goncalves Abrantes,[65] M. Goncerz,[41] G. Gong,[4,m] J. A. Gooding,[19] I. V. Gorelov,[44] C. Gotti,[31] E. Govorkova,[66] J. P. Grabowski,[30] L. A. Granado Cardoso,[50] E. Graugés,[46] E. Graverini,[35,51,u] L. Grazette,[58] G. Graziani,[27] A. T. Grecu,[43] N. A. Grieser,[67] L. Grillo,[61] S. Gromov,[44] C. Gu,[15] M. Guarise,[26] L. Guerry,[11] A.-K. Guseinov,[51] E. Gushchin,[44] Y. Guz,[6,50] T. Gys,[50] K. Habermann,[18] T. Hadavizadeh,[1] C. Hadjivasiliou,[68] G. Haefeli,[51] C. Haen,[50] S. Haken,[57] G. Hallett,[58] P. M. Hamilton,[68] J. Hammerich,[62] Q. Han,[33] X. Han,[22,50] S. Hansmann-Menzemer,[22] L. Hao,[7] N. Harnew,[65] T. H. Harris,[1] M. Hartmann,[14] S. Hashmi,[40] J. He,[7,t] N. Heatley,[14] A. Hedes,[64] F. Hemmer,[50] C. Henderson,[67] R. Henderson,[14] R. D. L. Henderson,[1] A. M. Hennequin,[50] K. Hennessy,[62] L. Henry,[51] J. Herd,[63] P. Herrero Gascon,[22] J. Heuel,[17] A. Heyn,[13] A. Hicheur,[3] G. Hijano Mendizabal,[52] J. Horswill,[64] R. Hou,[8] Y. Hou,[11] D. C. Houston,[61] N. Howarth,[62] W. Hu,[7] X. Hu,[4] W. Hulsbergen,[38] R. J. Hunter,[58] M. Hushchyn,[44] D. Hutchcroft,[62] M. Idzik,[40] D. Ilin,[44] P. Ilten,[67] A. Iniukhin,[44] A. Iohner,[10] A. Ishteev,[44] K. Ivshin,[44] H. Jage,[17] S. J. Jaimes Elles,[78,49,50] S. Jakobsen,[50] T. Jakoubek,[79] E. Jans,[38] B. K. Jashal,[49] A. Jawahery,[68] C. Jayaweera,[55] V. Jevtic,[19] Z. Jia,[16] E. Jiang,[68] X. Jiang,[5,7] Y. Jiang,[7] Y. J. Jiang,[6] E. Jimenez Moya,[9] N. Jindal,[89] M. John,[65] A. John Rubesh Rajan,[23] D. Johnson,[55] C. R. Jones,[57] S. Joshi,[42] B. Jost,[50] J. Juan Castella,[57] N. Jurik,[50] I. Juszczak,[41] K. Kalecinska,[40] D. Kaminaris,[51] S. Kandybei,[53] M. Kane,[60] Y. Kang,[4,m] C. Kar,[11] M. Karacson,[50] A. Kauniskangas,[51] J. W. Kautz,[67] M. K. Kazanecki,[41] F. Keizer,[50] M. Kenzie,[57] T. Ketel,[38] B. Khanji,[70] A. Kharisova,[44] S. Kholodenko,[63,50] G. Khreich,[14] T. Kirn,[17] V. S. Kirsebom,[31,c] S. Klaver,[39] N. Kleijne,[35,k] A. Kleimenova,[51] D. K. Klekots,[87] K. Klimaszewski,[42]

M. R. Kmiec,[42] T. Knospe,[19] R. Kolb,[22] S. Koliiev,[54] L. Kolk,[19] A. Konoplyannikov,[6] P. Kopciewicz,[50] P. Koppenburg,[38] A. Korchin,[53] M. Korolev,[44] I. Kostiuk,[38] O. Kot,[54] S. Kotriakhova,[32] E. Kowalczyk,[68] A. Kozachuk,[44] P. Kravchenko,[44] L. Kravchuk,[44] O. Kravcov,[82] M. Kreps,[58] P. Krokovny,[44] W. Krupa,[70] W. Krzemien,[42] O. Kshyvanskyi,[54] S. Kubis,[85] M. Kucharczyk,[41] V. Kudryavtsev,[44] E. Kulikova,[44] A. Kupsc,[86] V. Kushnir,[53] B. Kutsenko,[13] J. Kvapil,[69] I. Kyryllin,[53] D. Lacarrere,[50] P. Laguarta Gonzalez,[46] A. Lai,[32] A. Lampis,[32] D. Lancierini,[63] C. Landesa Gomez,[48] J. J. Lane,[1] G. Lanfranchi,[28] C. Langenbruch,[22] J. Langer,[19] T. Latham,[58] F. Lazzari,[35,50,u] C. Lazzeroni,[55] R. Le Gac,[13] H. Lee,[62] R. Lefèvre,[11] A. Leflat,[44] S. Legotin,[44] M. Lehuraux,[58] E. Lemos Cid,[50] O. Leroy,[13] T. Lesiak,[41] E. D. Lesser,[50] B. Leverington,[22] A. Li,[4,m] C. Li,[4,m] C. Li,[13] H. Li,[74] J. Li,[8] K. Li,[77] L. Li,[64] M. Li,[8] P. Li,[7] P.-R. Li,[75] Q. Li,[5,7] T. Li,[73] T. Li,[74] Y. Li,[8] Y. Li,[5] Y. Li,[4] Z. Lian,[4,m] Q. Liang,[8] X. Liang,[70] Z. Liang,[32] S. Libralon,[49] A. L. Lightbody,[12] C. Lin,[7] T. Lin,[59] R. Lindner,[50] H. Linton,[63] R. Litvinov,[32] D. Liu,[8] F. L. Liu,[1] G. Liu,[74] K. Liu,[75] S. Liu,[5] W. Liu,[8] Y. Liu,[60] Y. Liu,[75] Y. L. Liu,[63] G. Loachamin Ordonez,[71] I. Lobo,[1] A. Lobo Salvia,[46] A. Loi,[32] T. Long,[57] F. C. L. Lopes,[2,h] J. H. Lopes,[3] A. Lopez Huertas,[46] C. Lopez Iribarnegaray,[48] S. López Soliño,[48] Q. Lu,[15] C. Lucarelli,[50] D. Lucchesi,[33,v] M. Lucio Martinez,[49] Y. Luo,[6] A. Lupato,[33,w] E. Luppi,[26,g] K. Lynch,[23] X.-R. Lyu,[7] G. M. Ma,[4,m] H. Ma,[73] S. Maccolini,[19] F. Machefert,[14] F. Maciuc,[43] B. Mack,[70] I. Mackay,[65] L. M. Mackey,[70] L. R. Madhan Mohan,[57] M. J. Madurai,[55] D. Magdalinski,[38] D. Maisuzenko,[44] J. J. Malczewski,[41] S. Malde,[65] L. Malentacca,[50] A. Malinin,[44] T. Maltsev,[44] G. Manca,[32,o] G. Mancinelli,[13] C. Mancuso,[14] R. Manera Escalero,[46] F. M. Manganella,[37] D. Manuzzi,[25] D. Marangotto,[30,l] J. F. Marchand,[10] R. Marchevski,[51] U. Marconi,[25] E. Mariani,[16] S. Mariani,[50] C. Marin Benito,[46] J. Marks,[22] A. M. Marshall,[56] L. Martel,[65] G. Martelli,[34] G. Martellotti,[36] L. Martinazzoli,[50] M. Martinelli,[31,c] D. Martinez Gomez,[83] D. Martinez Santos,[45] F. Martinez Vidal,[49] A. Martorell i Granollers,[47] A. Massafferri,[2] R. Matev,[50] A. Mathad,[50] V. Matiunin,[44] C. Matteuzzi,[70] K. R. Mattioli,[15] A. Mauri,[63] E. Maurice,[15] J. Mauricio,[46] P. Mayencourt,[51] J. Mazorra de Cos,[49] M. Mazurek,[42] M. McCann,[63] N. T. McHugh,[61] A. McNab,[64] R. McNulty,[23] B. Meadows,[67] G. Meier,[19] D. Melnychuk,[42] D. Mendoza Granada,[16] P. Menendez Valdes Perez,[48] F. M. Meng,[4,m] M. Merk,[38,84] A. Merli,[51,30] L. Meyer Garcia,[68] D. Miao,[5,7] H. Miao,[7] M. Mikhasenko,[80] D. A. Milanes,[78,x] A. Minotti,[31,c] E. Minucci,[28] T. Miralles,[11] B. Mitreska,[64] D. S. Mitzel,[19] R. Mocanu,[43] A. Modak,[59] L. Moeser,[19] R. D. Moise,[17] E. F. Molina Cardenas,[88] T. Mombächer,[67] M. Monk,[57] T. Monnard,[51] S. Monteil,[11] A. Morcillo Gomez,[48] G. Morello,[28] M. J. Morello,[35,k] M. P. Morgenthaler,[22] A. Moro,[31,c] J. Moron,[40] W. Morren,[38] A. B. Morris,[50] A. G. Morris,[13] R. Mountain,[70] Z. M. Mu,[6] E. Muhammad,[58] F. Muheim,[60] M. Mulder,[83] K. Müller,[52] F. Muñoz-Rojas,[9] R. Murta,[63] V. Mytrochenko,[53] P. Naik,[62] T. Nakada,[51] R. Nandakumar,[59] T. Nanut,[50] G. Napoletano,[51] I. Nasteva,[3] M. Needham,[60] E. Nekrasova,[44] N. Neri,[30,l] S. Neubert,[18] N. Neufeld,[50] P. Neustroev,[44] J. Nicolini,[50] D. Nicotra,[84] E. M. Niel,[15] N. Nikitin,[44] L. Nisi,[19] Q. Niu,[75] P. Nogarolli,[3] P. Nogga,[18] C. Normand,[56] J. Novoa Fernandez,[48] G. Nowak,[67] C. Nunez,[88] H. N. Nur,[61] A. Oblakowska-Mucha,[40] V. Obraztsov,[44] T. Oeser,[17] A. Okhotnikov,[44] O. Okhrimenko,[54] R. Oldeman,[32,o] F. Oliva,[60,50] E. Olivart Pino,[46] M. Olocco,[19] R. H. O'Neil,[50] J. S. Ordonez Soto,[11] D. Osthues,[19] J. M. Otalora Goicochea,[3] P. Owen,[52] A. Oyanguren,[49] O. Ozcelik,[50] F. Paciolla,[35,y] A. Padee,[42] K. O. Padeken,[18] B. Pagare,[48] T. Pajero,[50] A. Palano,[24] L. Palini,[30] M. Palutan,[28] C. Pan,[76] X. Pan,[4,m] S. Panebianco,[12] S. Paniskaki,[50,33] G. Panshin,[5] L. Paolucci,[64] A. Papanestis,[59] M. Pappagallo,[24,q] L. L. Pappalardo,[26] C. Pappenheimer,[67] C. Parkes,[64] D. Parmar,[80] G. Passaleva,[27] D. Passaro,[35,50,k] A. Pastore,[24] M. Patel,[63] J. Patoc,[65] C. Patrignani,[25,i] A. Paul,[70] C. J. Pawley,[84] A. Pellegrino,[38] J. Peng,[5,7] X. Peng,[75] M. Pepe Altarelli,[28] S. Perazzini,[25] D. Pereima,[44] H. Pereira Da Costa,[69] M. Pereira Martinez,[48] A. Pereiro Castro,[48] C. Perez,[47] P. Perret,[11] A. Perrevoort,[83] A. Perro,[50,13] M. J. Peters,[67] K. Petridis,[56] A. Petrolini,[29,j] S. Pezzulo,[29,j] J. P. Pfaller,[67] H. Pham,[70] L. Pica,[35,k] M. Piccini,[34] L. Piccolo,[32] B. Pietrzyk,[10] G. Pietrzyk,[14] R. N. Pilato,[62] D. Pinci,[36] F. Pisani,[50] M. Pizzichemi,[31,50,c] V. M. Placinta,[43] M. Plo Casasus,[48] T. Poeschl,[50] F. Polci,[16] M. Poli Lener,[28] A. Poluektov,[13] N. Polukhina,[44] I. Polyakov,[64] E. Polycarpo,[3] S. Ponce,[50] D. Popov,[7,50] K. Popp,[19] S. Poslavskii,[44] K. Prasanth,[60] C. Prouve,[45] D. Provenzano,[32,50,o] V. Pugatch,[54] A. Puicercus Gomez,[50] G. Punzi,[35,u] J. R. Pybus,[69] Q. Q. Qian,[6] W. Qian,[7] N. Qin,[4,m] R. Quagliani,[50] R. I. Rabadan Trejo,[58] R. Racz,[82] J. H. Rademacker,[56] M. Rama,[35] M. Ramírez García,[88]

V. Ramos De Oliveira,[71] M. Ramos Pernas,[58] M. S. Rangel,[3] F. Ratnikov,[44] G. Raven,[39] M. Rebollo De Miguel,[49] F. Redi,[30,w] J. Reich,[56] F. Reiss,[20] Z. Ren,[7] P. K. Resmi,[65] M. Ribalda Galvez,[46] R. Ribatti,[51] G. Ricart,[12] D. Riccardi,[35,k] S. Ricciardi,[59] K. Richardson,[66] M. Richardson-Slipper,[57] F. Riehn,[19] K. Rinnert,[62] P. Robbe,[14,50] G. Robertson,[61] E. Rodrigues,[62] A. Rodriguez Alvarez,[46] E. Rodriguez Fernandez,[48] J. A. Rodriguez Lopez,[78] E. Rodriguez Rodriguez,[50] J. Roensch,[19] A. Rogachev,[44] A. Rogovskiy,[59] D. L. Rolf,[19] P. Roloff,[50] V. Romanovskiy,[67] A. Romero Vidal,[48] G. Romolini,[26,50] F. Ronchetti,[51] T. Rong,[6] M. Rotondo,[28] S. R. Roy,[22] M. S. Rudolph,[70] M. Ruiz Diaz,[22] R. A. Ruiz Fernandez,[48] J. Ruiz Vidal,[84] J. J. Saavedra-Arias,[9] J. J. Saborido Silva,[48] S. E. R. Sacha Emile R.,[50] N. Sagidova,[44] D. Sahoo,[81] N. Sahoo,[55] B. Saitta,[32] M. Salomoni,[31,50,c] I. Sanderswood,[49] R. Santacesaria,[36] C. Santamarina Rios,[48] M. Santimaria,[28] L. Santoro,[2] E. Santovetti,[37] A. Saputi,[26,50] D. Saranin,[44] A. Sarnatskiy,[83] G. Sarpis,[50] M. Sarpis,[82] C. Satriano,[36] A. Satta,[37] M. Saur,[75] D. Savrina,[44] H. Sazak,[17] F. Sborzacchi,[50,28] A. Scarabotto,[19] S. Schael,[17] S. Scherl,[62] M. Schiller,[22] H. Schindler,[50] M. Schmelling,[21] B. Schmidt,[50] N. Schmidt,[69] S. Schmitt,[66] H. Schmitz,[18] O. Schneider,[51] A. Schopper,[63] N. Schulte,[19] M. H. Schune,[14] G. Schwering,[17] B. Sciascia,[28] A. Sciuccati,[50] G. Scriven,[84] I. Segal,[80] S. Sellam,[48] A. Semennikov,[44] T. Senger,[52] M. Senghi Soares,[39] A. Sergi,[29,j] N. Serra,[52] L. Sestini,[27] A. Seuthe,[19] B. Sevilla Sanjuan,[47] Y. Shang,[6] D. M. Shangase,[88] M. Shapkin,[44] R. S. Sharma,[70] I. Shchemerov,[44] L. Shchutska,[51] T. Shears,[62] L. Shekhtman,[44] Z. Shen,[38] S. Sheng,[5,7] V. Shevchenko,[44] B. Shi,[7] Q. Shi,[7] W. S. Shi,[74] Y. Shimizu,[14] E. Shmanin,[25] R. Shorkin,[44] J. D. Shupperd,[70] R. Silva Coutinho,[2] G. Simi,[33,v] S. Simone,[24,q] M. Singha,[81] N. Skidmore,[58] T. Skwarnicki,[70] M. W. Slater,[55] E. Smith,[66] K. Smith,[69] M. Smith,[63] L. Soares Lavra,[60] M. D. Sokoloff,[67] F. J. P. Soler,[61] A. Solomin,[56] A. Solovev,[44] K. Solovieva,[20] N. S. Sommerfeld,[18] R. Song,[1] Y. Song,[51] Y. Song,[4,m] Y. S. Song,[6] F. L. Souza De Almeida,[46] B. Souza De Paula,[3] K. M. Sowa,[40] E. Spadaro Norella,[29,j] E. Spedicato,[25] J. G. Speer,[19] P. Spradlin,[61] F. Stagni,[50] M. Stahl,[80] S. Stahl,[50] S. Stanislaus,[65] M. Stefaniak,[89] E. N. Stein,[50] O. Steinkamp,[52] D. Strekalina,[44] Y. Su,[7] F. Suljik,[65] J. Sun,[32] J. Sun,[64] L. Sun,[76] D. Sundfeld,[2] W. Sutcliffe,[52] P. Svihra,[79] V. Svintozelskyi,[49] K. Swientek,[40] F. Swystun,[57] A. Szabelski,[42] T. Szumlak,[40] Y. Tan,[4] Y. Tang,[76] Y. T. Tang,[7] M. D. Tat,[22] J. A. Teijeiro Jimenez,[48] A. Terentev,[44] F. Terzuoli,[35,y] F. Teubert,[50] E. Thomas,[50] D. J. D. Thompson,[55] A. R. Thomson-Strong,[60] H. Tilquin,[63] V. Tisserand,[11] S. T'Jampens,[10] M. Tobin,[5,50] T. T. Todorov,[20] L. Tomassetti,[26,g] G. Tonani,[30] X. Tong,[6] T. Tork,[30] D. Torres Machado,[2] L. Toscano,[19] D. Y. Tou,[4,m] C. Trippl,[47] G. Tuci,[22] N. Tuning,[38] L. H. Uecker,[22] A. Ukleja,[40] D. J. Unverzagt,[22] A. Upadhyay,[50] B. Urbach,[60] A. Usachov,[38] A. Ustyuzhanin,[44] U. Uwer,[22] V. Vagnoni,[25,50] A. Vaitkevicius,[82] V. Valcarce Cadenas,[48] G. Valenti,[25] N. Valls Canudas,[50] J. van Eldik,[50] H. Van Hecke,[69] E. van Herwijnen,[63] C. B. Van Hulse,[48,z] R. Van Laak,[51] M. van Veghel,[84] G. Vasquez,[52] R. Vazquez Gomez,[46] P. Vazquez Regueiro,[48] C. Vázquez Sierra,[45] S. Vecchi,[26] J. Velilla Serna,[49] J. J. Velthuis,[56] M. Veltri,[27,aa] A. Venkateswaran,[51] M. Verdoglia,[32] M. Vesterinen,[58] W. Vetens,[70] D. Vico Benet,[65] P. Vidrier Villalba,[46] M. Vieites Diaz,[48] X. Vilasis-Cardona,[47] E. Vilella Figueras,[62] A. Villa,[25] P. Vincent,[16] B. Vivacqua,[3] F. C. Volle,[55] D. vom Bruch,[13] N. Voropaev,[44] K. Vos,[84] C. Vrahas,[60] J. Wagner,[19] J. Walsh,[35] E. J. Walton,[1,58] G. Wan,[6] A. Wang,[7] B. Wang,[5] C. Wang,[22] G. Wang,[8] H. Wang,[75] J. Wang,[7] J. Wang,[5] J. Wang,[4,m] J. Wang,[76] M. Wang,[50] N. W. Wang,[7] R. Wang,[56] X. Wang,[8] X. Wang,[74] X. W. Wang,[63] Y. Wang,[77] Y. Wang,[6] Y. H. Wang,[75] Z. Wang,[14] Z. Wang,[30] J. A. Ward,[58,1] M. Waterlaat,[50] N. K. Watson,[55] D. Websdale,[63] Y. Wei,[6] Z. Weida,[7] J. Wendel,[45] B. D. C. Westhenry,[56] C. White,[57] M. Whitehead,[61] E. Whiter,[55] A. R. Wiederhold,[64] D. Wiedner,[19] M. A. Wiegertjes,[38] C. Wild,[65] G. Wilkinson,[65,50] M. K. Wilkinson,[67] M. Williams,[66] M. J. Williams,[50] M. R. J. Williams,[60] R. Williams,[57] S. Williams,[56] Z. Williams,[56] F. F. Wilson,[59] M. Winn,[12] W. Wislicki,[42] M. Witek,[41] L. Witola,[19] T. Wolf,[22] E. Wood,[57] G. Wormser,[14] S. A. Wotton,[57] H. Wu,[70] J. Wu,[8] X. Wu,[76] Y. Wu,[6,57] Z. Wu,[7] K. Wyllie,[50] S. Xian,[74] Z. Xiang,[5] Y. Xie,[8] T. X. Xing,[30] A. Xu,[35,k] L. Xu,[4,m] M. Xu,[50] Z. Xu,[50] Z. Xu,[7] Z. Xu,[5] S. Yadav,[26] K. Yang,[63] X. Yang,[6] Y. Yang,[7] Y. Yang,[81] Z. Yang,[6] V. Yeroshenko,[14] H. Yeung,[64] H. Yin,[8] X. Yin,[7] C. Y. Yu,[6] J. Yu,[73] X. Yuan,[5] Y Yuan,[5,7] J. A. Zamora Saa,[72] M. Zavertyaev,[21] M. Zdybal,[41] F. Zenesini,[25] C. Zeng,[5,7] M. Zeng,[4,m] C. Zhang,[6] D. Zhang,[8] J. Zhang,[7] L. Zhang,[4,m] R. Zhang,[8] S. Zhang,[65] S. L. Zhang,[73] Y. Zhang,[6] Y. Z. Zhang,[4,m] Z. Zhang,[4,m] Y. Zhao,[22] A. Zhelezov,[22] S. Z. Zheng,[6]

X. Z. Zheng,[4,m] Y. Zheng,[7] T. Zhou,[6] X. Zhou,[8] Y. Zhou,[7] V. Zhovkovska,[58] L. Z. Zhu,[7] X. Zhu,[4,m] X. Zhu,[8] Y. Zhu,[17] V. Zhukov,[17] J. Zhuo,[49] Q. Zou,[5,7] D. Zuliani,[33,v] and G. Zunica[28]

(LHCb Collaboration)

[1]*School of Physics and Astronomy, Monash University, Melbourne, Australia*
[2]*Centro Brasileiro de Pesquisas Físicas (CBPF), Rio de Janeiro, Brazil*
[3]*Universidade Federal do Rio de Janeiro (UFRJ), Rio de Janeiro, Brazil*
[4]*Department of Engineering Physics, Tsinghua University, Beijing, China*
[5]*Institute of High Energy Physics (IHEP), Beijing, China*
[6]*School of Physics State Key Laboratory of Nuclear Physics and Technology, Peking University, Beijing, China*
[7]*University of Chinese Academy of Sciences, Beijing, China*
[8]*Institute of Particle Physics, Central China Normal University, Wuhan, Hubei, China*
[9]*Consejo Nacional de Rectores (CONARE), San Jose, Costa Rica*
[10]*Université Savoie Mont Blanc, CNRS, IN2P3-LAPP, Annecy, France*
[11]*Université Clermont Auvergne, CNRS/IN2P3, LPC, Clermont-Ferrand, France*
[12]*Université Paris-Saclay, Centre d'Etudes de Saclay (CEA), IRFU, Saclay, France, Gif-Sur-Yvette, France*
[13]*Aix Marseille Univ, CNRS/IN2P3, CPPM, Marseille, France*
[14]*Université Paris-Saclay, CNRS/IN2P3, IJCLab, Orsay, France*
[15]*Laboratoire Leprince-Ringuet, CNRS/IN2P3, Ecole Polytechnique, Institut Polytechnique de Paris, Palaiseau, France*
[16]*Laboratoire de Physique Nucléaire et de Hautes Énergies (LPNHE), Sorbonne Université, CNRS/IN2P3, F-75005 Paris, France, Paris, France*
[17]*I. Physikalisches Institut, RWTH Aachen University, Aachen, Germany*
[18]*Universität Bonn - Helmholtz-Institut für Strahlen und Kernphysik, Bonn, Germany*
[19]*Fakultät Physik, Technische Universität Dortmund, Dortmund, Germany*
[20]*Physikalisches Institut, Albert-Ludwigs-Universität Freiburg, Freiburg, Germany*
[21]*Max-Planck-Institut für Kernphysik (MPIK), Heidelberg, Germany*
[22]*Physikalisches Institut, Ruprecht-Karls-Universität Heidelberg, Heidelberg, Germany*
[23]*School of Physics, University College Dublin, Dublin, Ireland*
[24]*INFN Sezione di Bari, Bari, Italy*
[25]*INFN Sezione di Bologna, Bologna, Italy*
[26]*INFN Sezione di Ferrara, Ferrara, Italy*
[27]*INFN Sezione di Firenze, Firenze, Italy*
[28]*INFN Laboratori Nazionali di Frascati, Frascati, Italy*
[29]*INFN Sezione di Genova, Genova, Italy*
[30]*INFN Sezione di Milano, Milano, Italy*
[31]*INFN Sezione di Milano-Bicocca, Milano, Italy*
[32]*INFN Sezione di Cagliari, Monserrato, Italy*
[33]*INFN Sezione di Padova, Padova, Italy*
[34]*INFN Sezione di Perugia, Perugia, Italy*
[35]*INFN Sezione di Pisa, Pisa, Italy*
[36]*INFN Sezione di Roma La Sapienza, Roma, Italy*
[37]*INFN Sezione di Roma Tor Vergata, Roma, Italy*
[38]*Nikhef National Institute for Subatomic Physics, Amsterdam, Netherlands*
[39]*Nikhef National Institute for Subatomic Physics and VU University Amsterdam, Amsterdam, Netherlands*
[40]*AGH - University of Krakow, Faculty of Physics and Applied Computer Science, Kraków, Poland*
[41]*Henryk Niewodniczanski Institute of Nuclear Physics Polish Academy of Sciences, Kraków, Poland*
[42]*National Center for Nuclear Research (NCBJ), Warsaw, Poland*
[43]*Horia Hulubei National Institute of Physics and Nuclear Engineering, Bucharest-Magurele, Romania*
[44]*Authors affiliated with an institute formerly covered by a cooperation agreement with CERN*
[45]*Universidade da Coruña, A Coruña, Spain*
[46]*ICCUB, Universitat de Barcelona, Barcelona, Spain*
[47]*La Salle, Universitat Ramon Llull, Barcelona, Spain*
[48]*Instituto Galego de Física de Altas Enerxías (IGFAE), Universidade de Santiago de Compostela, Santiago de Compostela, Spain*
[49]*Instituto de Fisica Corpuscular, Centro Mixto Universidad de Valencia—CSIC, Valencia, Spain*
[50]*European Organization for Nuclear Research (CERN), Geneva, Switzerland*
[51]*Institute of Physics, Ecole Polytechnique Fédérale de Lausanne (EPFL), Lausanne, Switzerland*
[52]*Physik-Institut, Universität Zürich, Zürich, Switzerland*

[53]NSC Kharkiv Institute of Physics and Technology (NSC KIPT), Kharkiv, Ukraine
[54]Institute for Nuclear Research of the National Academy of Sciences (KINR), Kyiv, Ukraine
[55]School of Physics and Astronomy, University of Birmingham, Birmingham, United Kingdom
[56]H.H. Wills Physics Laboratory, University of Bristol, Bristol, United Kingdom
[57]Cavendish Laboratory, University of Cambridge, Cambridge, United Kingdom
[58]Department of Physics, University of Warwick, Coventry, United Kingdom
[59]STFC Rutherford Appleton Laboratory, Didcot, United Kingdom
[60]School of Physics and Astronomy, University of Edinburgh, Edinburgh, United Kingdom
[61]School of Physics and Astronomy, University of Glasgow, Glasgow, United Kingdom
[62]Oliver Lodge Laboratory, University of Liverpool, Liverpool, United Kingdom
[63]Imperial College London, London, United Kingdom
[64]Department of Physics and Astronomy, University of Manchester, Manchester, United Kingdom
[65]Department of Physics, University of Oxford, Oxford, United Kingdom
[66]Massachusetts Institute of Technology, Cambridge, Massachusetts, USA
[67]University of Cincinnati, Cincinnati, Ohio, USA
[68]University of Maryland, College Park, Maryland, USA
[69]Los Alamos National Laboratory (LANL), Los Alamos, New Mexico, USA
[70]Syracuse University, Syracuse, New York, USA
[71]Pontifícia Universidade Católica do Rio de Janeiro (PUC-Rio), Rio de Janeiro, Brazil (associated with Universidade Federal do Rio de Janeiro (UFRJ), Rio de Janeiro, Brazil)
[72]Universidad Andres Bello, Santiago, Chile (associated with Physik-Institut, Universität Zürich, Zürich, Switzerland)
[73]School of Physics and Electronics, Hunan University, Changsha City, China (associated with Institute of Particle Physics, Central China Normal University, Wuhan, Hubei, China)
[74]Guangdong Provincial Key Laboratory of Nuclear Science, Guangdong-Hong Kong Joint Laboratory of Quantum Matter, Institute of Quantum Matter, South China Normal University, Guangzhou, China (associated with Department of Engineering Physics, Tsinghua University, Beijing, China)
[75]Lanzhou University, Lanzhou, China (associated with Institute of High Energy Physics (IHEP), Beijing, China)
[76]School of Physics and Technology, Wuhan University, Wuhan, China (associated with Department of Engineering Physics, Tsinghua University, Beijing, China)
[77]Henan Normal University, Xinxiang, China (associated with Institute of Particle Physics, Central China Normal University, Wuhan, Hubei, China)
[78]Departamento de Fisica, Universidad Nacional de Colombia, Bogota, Colombia (associated with Laboratoire de Physique Nucléaire et de Hautes Énergies (LPNHE), Sorbonne Université, CNRS/IN2P3, F-75005 Paris, France, Paris, France)
[79]Institute of Physics of the Czech Academy of Sciences, Prague, Czech Republic (associated with Department of Physics and Astronomy, University of Manchester, Manchester, United Kingdom)
[80]Ruhr Universitaet Bochum, Fakultaet f. Physik und Astronomie, Bochum, Germany (associated with Fakultät Physik, Technische Universität Dortmund, Dortmund, Germany)
[81]Eotvos Lorand University, Budapest, Hungary (associated with European Organization for Nuclear Research (CERN), Geneva, Switzerland)
[82]Faculty of Physics, Vilnius University, Vilnius, Lithuania (associated with Physikalisches Institut, Albert-Ludwigs-Universität Freiburg, Freiburg, Germany)
[83]Van Swinderen Institute, University of Groningen, Groningen, Netherlands (associated with Nikhef National Institute for Subatomic Physics, Amsterdam, Netherlands)
[84]Universiteit Maastricht, Maastricht, Netherlands (associated with Nikhef National Institute for Subatomic Physics, Amsterdam, Netherlands)
[85]Tadeusz Kosciuszko Cracow University of Technology, Cracow, Poland (associated with Henryk Niewodniczanski Institute of Nuclear Physics Polish Academy of Sciences, Kraków, Poland)
[86]Department of Physics and Astronomy, Uppsala University, Uppsala, Sweden (associated with School of Physics and Astronomy, University of Glasgow, Glasgow, United Kingdom)
[87]Taras Schevchenko University of Kyiv, Faculty of Physics, Kyiv, Ukraine (associated with Université Paris-Saclay, CNRS/IN2P3, IJCLab, Orsay, France)
[88]University of Michigan, Ann Arbor, Michigan, USA (associated with Syracuse University, Syracuse, New York, USA)
[89]Ohio State University, Columbus, USA (associated with Los Alamos National Laboratory (LANL), Los Alamos, New Mexico, USA)

[a]Deceased.
[b]Also at Lamarr Institute for Machine Learning and Artificial Intelligence, Dortmund, Germany.
[c]Also at Università degli Studi di Milano-Bicocca, Milano, Italy.
[d]Also at Università di Roma Tor Vergata, Roma, Italy.

[e]Also at Università di Modena e Reggio Emilia, Modena, Italy.
[f]Also at Department of Physics and Astronomy, University of Victoria, Victoria, Canada.
[g]Also at Università di Ferrara, Ferrara, Italy.
[h]Also at Universidade Estadual de Campinas (UNICAMP), Campinas, Brazil.
[i]Also at Università di Bologna, Bologna, Italy.
[j]Also at Università di Genova, Genova, Italy.
[k]Also at Scuola Normale Superiore, Pisa, Italy.
[l]Also at Università degli Studi di Milano, Milano, Italy.
[m]Also at Center for High Energy Physics, Tsinghua University, Beijing, China.
[n]Also at Universidad Nacional Autónoma de Honduras, Tegucigalpa, Honduras.
[o]Also at Università di Cagliari, Cagliari, Italy.
[p]Also at Centro Federal de Educacão Tecnológica Celso Suckow da Fonseca, Rio De Janeiro, Brazil.
[q]Also at Università di Bari, Bari, Italy.
[r]Also at Università di Perugia, Perugia, Italy.
[s]Also at LIP6, Sorbonne Université, Paris, France.
[t]Also at Hangzhou Institute for Advanced Study, UCAS, Hangzhou, China.
[u]Also at Università di Pisa, Pisa, Italy.
[v]Also at Università di Padova, Padova, Italy.
[w]Also at Università di Bergamo, Bergamo, Italy.
[x]Also at Universidad de Ingeniería y Tecnología (UTEC), Lima, Peru.
[y]Also at Università di Siena, Siena, Italy.
[z]Also at Universidad de Alcalá, Alcalá de Henares, Spain.
[aa]Also at Università di Urbino, Urbino, Italy.